Influence of ZnO addition on the sintering properties of SnO$_2$ electrodes

Jie Liu · Wei Ning

Abstract The effect of ZnO doping in SnO$_2$ was investigated for electrodes. Zinc oxide in different concentration, 0.5–5 wt%, was added to tin dioxide powder prepared by a coprecipitation method. The products were characterized by powder X-ray diffraction, transmission electron microscopy, and by section scanning electron microscopy. The resistivity of those electrodes was measured with KEITHLEY236 high-resistance instrument. It was found that ZnO was expected to increase the electrical conductivity of SnO$_2$ ceramic. However, the range of solid solution of ZnO into SnO$_2$ lattice was found to be limited as it rapidly segregated to form secondary phases. Concentrations as high as 5 wt% of ZnO lead to the formation of a ZnSnO$_3$ phase whose presence yielded a non-linear electrical response that hinders the donor effect of zinc oxide.

Introduction

Much interest has focused on obtaining dense SnO$_2$ ceramics for applications such as varistors [1], photochemical devices [2], and components requiring high chemical corrosion resistance. However, tin dioxide electrodes used in the electric glass-melting furnace [3] have been barely mentioned. Tin dioxide is a semiconductor (n-type) with wide band gap. It shows poor sinterability and sintering aids have been used to promote densification. Several authors have studied the effect of different oxides such as CoO [4, 5], CuO [6], MnO$_2$ [5], Bi$_2$O$_3$ [7], Sb$_2$O$_3$ [8], In$_2$O$_3$ [9], and Nb$_2$O$_5$

J. Liu (✉) · W. Ning
College of Material Science and Engineering, Donghua University, 200051 Shanghai, People's Republic of China
e-mail: jerray2008@163.com

[10] in SnO$_2$ sintering. In recent years, SnO$_2$ dense ceramics can be obtained by the introduction of densifying agents, such as ZnO [3], which promote the densification of SnO$_2$ almost to 92% of the theoretical value and improve the electrical conductivity of SnO$_2$. But few reports describe the effect of sintering atmospheres or the role of ZnO on SnO$_2$ sintering. Foschini et al. [3] studied the sintering of tin oxide using zinc oxide as a densification aid and found that ZnO acts as a densifying agent for SnO$_2$ through the oxygen vacancy formation mechanism. Quadir and Readey [11] observed that sintering SnO$_2$ in a hydrogen atmosphere caused the compact to expand, decreasing its apparent density, and that the behavior of exaggerated particle growth was non-isotropic. They found that the expansion process was caused by agglomerate grain growth due to evaporation condensation at temperatures above 1,200 °C, which is given by the Eq. 1:

$$SnO_{2(S)} \rightarrow SnO + \frac{1}{2}O_2. \tag{1}$$

Perazolli et al. [12, 13] studied the influence of the atmosphere on SnO$_2$ plus ZnO sintering, verifying that Zn promotes densification due the formation of oxygen vacancies in the structure, which is expressed by the Eq. 2:

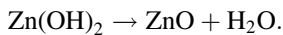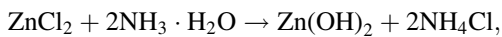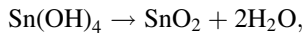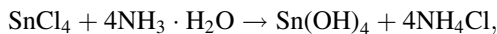$$ZnO \overset{SnO_2}{\rightarrow} Zn_{Sn}^{''} + V_O^{\bullet\bullet} + O_O^{\times}. \tag{2}$$

The present study involved an investigation of influence of ZnO addition on the sintering properties of SnO$_2$ electrodes. The fracture surface of sintered samples was analyzed by scanning electron microscopy (SEM), while the grain boundary precipitates formed at the grain boundaries in compositions with 10 wt% ZnO were analyzed by EDS. The predominant densification mechanism is suggested here, as is the probable formation of a ZnSnO$_3$ phase at the grain boundaries.

Experimental procedure

The nanosized ZnO-doped SnO_2 powders were prepared using the coprecipitation method. $SnCl_4 \cdot 5H_2O$ and $ZnCl_2$ (analytic reagent grade, or A.R.) were used as the starting materials, and $NH_3 \cdot H_2O$ was used as the coprecipitant without further purification. The formation of SnO_2 and ZnO are a two-stage process:

$$SnCl_4 + 4NH_3 \cdot H_2O \rightarrow Sn(OH)_4 + 4NH_4Cl,$$

$$Sn(OH)_4 \rightarrow SnO_2 + 2H_2O,$$

$$ZnCl_2 + 2NH_3 \cdot H_2O \rightarrow Zn(OH)_2 + 2NH_4Cl,$$

$$Zn(OH)_2 \rightarrow ZnO + H_2O.$$

The SnO_2-based materials were doped with various quantities of ZnO: 0.5, 1.0, 1.5, 2.0, 2.5, 3.0, and 5.0 wt%. Accordingly, $ZnCl_2$ and $SnCl_4 \cdot 5H_2O$ in above mass ratio were dissolved in a minimum amount of deionized water for the preparation of ZnO-doped SnO_2 powders. Then the $4 \ mol \ L^{-1} \ NH_3 \cdot H_2O$ solution was added, respectively, into the above solutions to adjust the pH to about 7, and the white amorphous precipitates were formed. The precipitates were filtered and washed with deionized water until no Cl^- were found in the filtrates. Then, the wet powders were dried at about 80 °C in air to form the precursors of ZnO-doped SnO_2 powders. Finally, the precursors were calcined at 600 °C in air to prepare the nanosized powders.

Some powders were pressed into pellets by uniaxial pressing followed by isostatic pressing at 210 MPa. No calcination was performed prior to the pellet preparation. These pellets were then sintered for 4 h in dynamic oxygen atmosphere (flux 3 cm^3/min, oxygen purity 95%) at optimized maximum sintering temperatures, which were obtained from dilatometry of the different compositions and are given in Table 1. All heating rates were 5 °C/min; the samples were slowly cooled to room temperature (cooling rate 5 °C/min). The dilatometric analyses were performed with a Netzsch 402E unit, up to 1,500 °C, at a heating rate of 10 °C/min in oxygen atmosphere. The linear shrinkage and linear shrinkage rates were collected every 0.5 °C.

The tin dioxide electrodes were made by the nanosized ZnO-doped SnO_2 powders under 25 KN pressure, and sintered in air at 1,300 °C. Cross-sections of the electrodes were mechanically ground and polished. Ground powders were characterized by X-ray powder diffraction (XRD) in 2θ range from 20° to 85° using Brucker Analytical X-ray diffractometer equipped with graphite monochromatized CuK_α radiation ($\lambda = 1.5418$ Å). The microstructures of polished electrodes were examined using a scanning electron microscope (SEM; JSM-5600LV, Jeol) equipped with X-ray spectrometer (EDS; Link IE300X, Oxford Instruments).

Table 1 Dilatometric results obtained during the sintering of SnO_2–ZnO samples at a constant heating rate

ZnO content (wt%)	T_{sd} (°C)	T_{max} (°C)	G (μm)	ρ (%)
0.5	855	1,250	4.6	95.1
1.0	780	1,125	5.2	97.2
2.0	760	1,160	6.6	98.4
3.0	750	1,195	10.3	98.1
5.0	745	1,210	6.2	97.5

T_{sd} is the temperature at which densification begins; T_{max} is the temperature at which the shrinkage rate is at its maximum; G is the mean grain size; and ρ is the relative density

Results and discussion

Figure 1 shows XRD patterns of some tin dioxide electrodes considered in this study. Samples containing less than 1 wt% ZnO did not exhibit the presence of any precipitate at the grain boundaries, indicating the formation of solid solution between ZnO and SnO_2. It can be observed that grains and simple grain boundaries mainly consist of SnO_2 while the grain boundaries are Zn enriched. It was also found that the precipitates contain a high concentration of dopants. From these results, we can confirm that Zn segregates at the grain boundaries. It is suggested that the addition of 5 wt% ZnO causes a $ZnSnO_3$ phase segregation at the grain boundaries due to the substitution of Zn by Sn.

The influence of ZnO dopants on the sintering process of the SnO_2 electrodes were investigated by dilatometric analyses. It was observed that the ZnO addition affects the
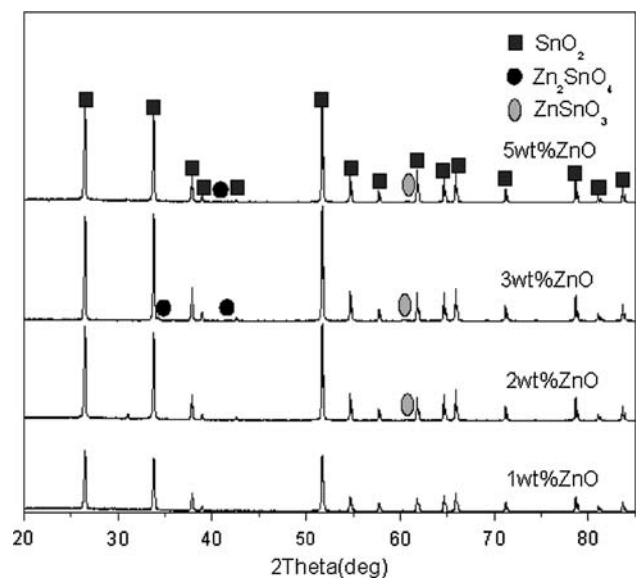
Fig. 1 XRD patterns of ZnO-doped SnO_2 samples with different ZnO contents

grain size and the final density of the sintered samples (Table 1). The linear shrinkage rate $(d(\Delta l/l_0)/dt)$ and linear shrinkage $(\Delta l/l_0)$ as a function of temperature for different ZnO concentrations were presented in Fig. 2a and b. The results shown in Fig. 2a and b indicated that the ceramic powder obtained did not react chemically in the temperature range and that the peaks occurring around 1,200 °C (Fig. 2a) were attributable to a stannic reduction, according to Eq. 1. The weight loss occurring above 1,200 °C was due to the reduction of SnO_2 to SnO (Eq. 1). The addition of ZnO led to the formation of oxygen vacancies (Eq. 2) that competed with the O_2 formed, inhibiting the formation of SnO, according to Eq. 1, and the starting temperature of weight loss shifted from 1,200 to 1300 °C. A constant weight gain occurred due to the absorption of O_2 up to 1,300 °C, after which the weight loss up to 1,500 °C was less than 1% in mass, due to the evaporation of SnO_2. It was noted that the densification temperature decreases with an increasing ZnO concentration due to a higher amount of O vacancies, according to the equation 2. These vacancies facilitate material diffusion during sintering. Figure 2b illustrates the linear

Fig. 2 Dilatometric results obtained from ZnO-doped SnO_2 sintered at a 10 °C/min heating rate up to 1,500 °C in dry air: **a** linear shrinkage (%) and **b** linear shrinkage rate (min^{-1})

shrinkage rate for different ZnO concentrations. From these results, it can be verified that the limit to form a ZnO solid solution in the SnO_2 matrix is 3 wt%. The initial sintering temperature (T_{sd}), the maxium sintering temperature (T_{max}), the mean grain size (G), and the relative density (ρ) are given in Table 1. The increase in zinc concentration has strong influence on the sintering process of the system. For the highly doped samples, there is a segregation at the grain boundaries, which leads to a decrease in the grain size. This effect is mainly due to the precipitation of a new enriched ceramic phase, as discussed in the subsequent sections. The bulk densities of the samples determined by Archimedes method were evaluated as a function of ZnO content and are related to the theoretical density of SnO_2 ($\rho_{theoretical} = 6.95$ g/cm^3). The highest values were obtained for the compositions SnO_2 + 3 wt% ZnO ($\rho > 98\%$). The final densities after sintering are close to 95%, as shown in Table 1. A dramatic decrease in grain size was also noted for the heavily 5 wt% ZnO-doped samples. This indicates that Zn in higher concentrations not only provides oxygen vacancies to facilitate the densification, but also acts as a grain growth inhibitor. This could result in a $ZnSnO_3$ phase at the grain boundaries.

Figure 3 shows SEM images of some tin dioxide electrodes considered in this study. The mean grain size was obtained by the intercept method. The samples doped with 5 wt% ZnO presented a larger number of pores (intergranulars and intragranulars) compared with the samples doped with 2 wt% ZnO (intergranulars and intragranulars). And the samples doped with 3 wt% ZnO presented some spheroidal grains (intergranulars and intragranulars) compared with the samples doped with 1 wt% ZnO (intergranulars and intragranulars). There are significant differences in the average grain size with the addition of ZnO probably due to the segregation of a $ZnSnO_3$ phase at the grain boundaries, which might decrease the grain boundary mobility leading to a decrease in the grain size.

An analysis was made of the composition of the grain boundary inclusions using EDS coupled to a SEM micrograph. Figure 4a and b show a micrograph and an energy dispersive spectrum of a sample containing 5 wt% ZnO. A chemical analysis of the grains in these samples revealed a ZnO-rich phase, as illustrated in Fig. 1 and this ZnO-rich phase was identified as $ZnSnO_3$.

Current–voltage measurements as function of ZnO content and sintering time were presented in Fig. 5a and b, respectively. The addition of ZnO reduced the room temperature resistivity from 1,000 kΩ cm (pure undoped SnO_2) to 35 kΩ cm (system SnO_2 + 3 wt% ZnO). It was confirmed that the sintering time also influences the resistivity, for 2 h sintering time, the highest value was obtained (Fig. 5b). In order to optimize these ceramics for technical applications, attention should be paid to this fact. The
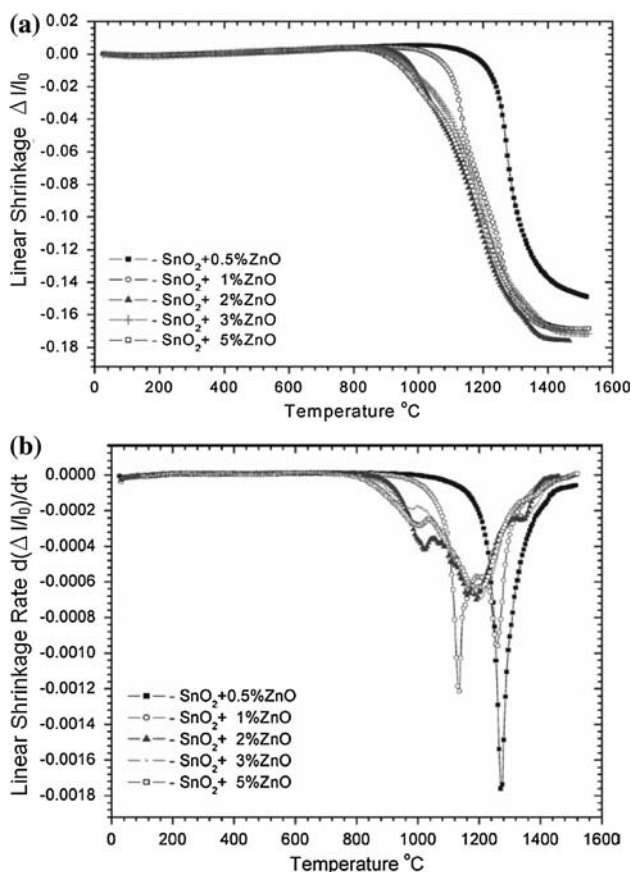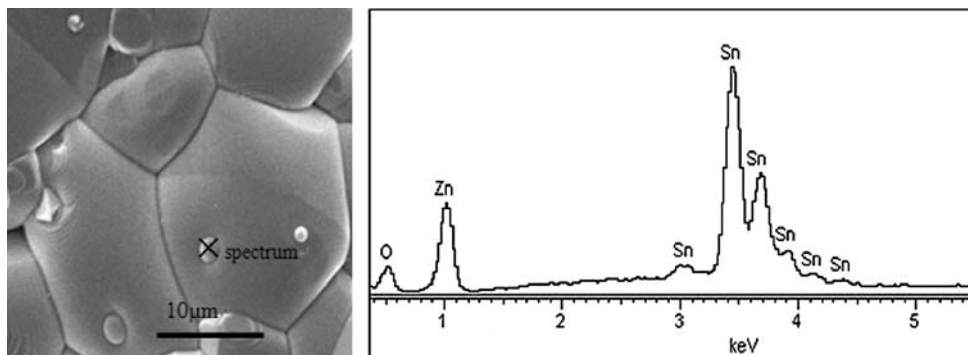
Fig. 3 SEM micrographs of fractured samples with ZnO content of: **a** 1 wt%, **b** 2 wt%, **c** 3 wt%, and **d** 5 wt%
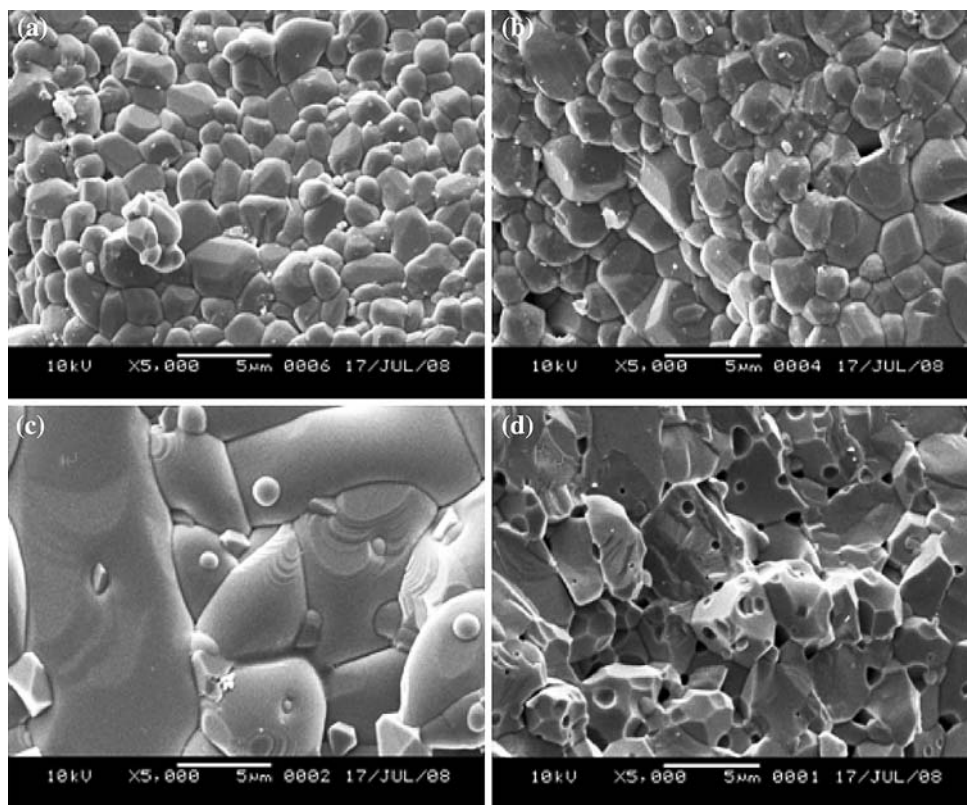
Fig. 4 SEM micrograph and EDS spectrum of a sample containing 5 wt% ZnO


previously discussed segregation of ZnO at the grain boundaries is responsible for the increase in the electric resistivity of the SnO_2–ZnO system, which really improve the resistivity of tin dioxide electrodes. But these results prove that the optimized tin dioxide is still a semiconductor.

Conclusions

The addition of ZnO to SnO_2, with the development of $ZnSnO_3$, showed a dramatic effect on the microstruture. The

main mechanism for inhibiting grain growth was the pinning of grain boundaries due to the presence of the $ZnSnO_3$ particles. Incorporation of a small amount of ZnO (1 wt% < ZnO ≤ 3 wt%) led to a marked increase in both the electrical conductivity and the bulk density of the SnO_2 electrodes. On the other hand, samples with higher ZnO content (ZnO ≥ 5 wt%) displayed the presence of a $ZnSnO_3$ phase precipitated at the grain boundaries, which may act as a barrier for grain mobility, inhibiting densification and grain growth.
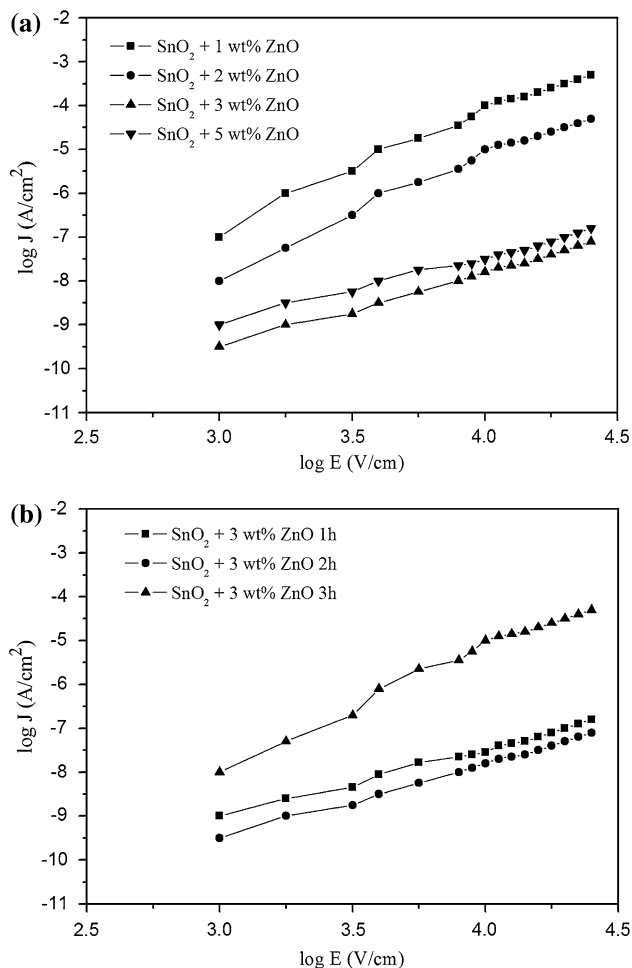
Fig. 5 Applied electric field as a function of current density for different ZnO concentrations (**a**) and sintering times (**b**)

References

1. Wang JF, Wang YJ, Su WB, Chen HC, Wang WX (2002) Mater Sci Eng B 96:8
2. Wang C, Wang XM, Xu BQ, Zhao JC, Mai BX, Peng PA, Sheng GY, Fu JM (2004) J Photochem Photobiol A Chem 168:47
3. Foschini CR, Perazolli L, Varela JA (2004) J Mater Sci 39(18):5825. doi:10.1023/B:JMSC.0000040095.03906.61
4. Varela JA, Cerri JA, Leite ER, Longo E, Shamsuzzoha M, Bradt RC (1999) Ceram Int 25:253
5. Dibb A, Tebcherani SM, Lacerda W Jr, Santos MRC, Cilense M, Varela JA, Longo E (2000) Mater Lett 46:39
6. Bonnet JP, Dolet N, Heintz JM (1996) J Eur Ceram Soc 16:1163
7. Muraoka M, Suzuki M, Sawada Y, Matsushita J (1998) J Mater Sci 33:5621. doi:10.1023/A:1004420416545
8. Hu YH, Zhang HH, Yang HM (2008) J Alloy Compd 453:292
9. Zang GZ, Wang JF, Chen HC, Su WB, Wang WX, Wang CM, Qi P (2005) J Non-Cryst Solids 351:941
10. Brankovica G, Brankovica Z, Davolos MR, Cilense M, Varela JA (2004) Mater Character 52:243
11. Quadir T, Readey DW (2005) J Am Ceram Soc 72:297
12. Perazolli L, Foschini CR, Giraldi TR, Biscaro RS, Varela JA, Longo E (2000) Sinter Sci Technol 117
13. Perazolli L, Varela JA, Leite ER, Longo E (1999) Mater Sci Forum 299/300:134